



Article

Effects of Large- and Meso-Scale Circulation on Uprising Dust over Bodélé in June 2006 and June 2011

Ridha Guebsi and Karem Chokmani

Special Issue

Advances in Remote Sensing Observation of Aerosol Properties and Assessment of Their Effects



Edited by

Dr. Kaitao Li, Dr. Xingfeng Chen, Dr. Lei Li and Dr. Donghui Li



Article

Effects of Large- and Meso-Scale Circulation on Uprising Dust over Bodélé in June 2006 and June 2011

Ridha Guebsi *  and Karem Chokmani 

Centre Eau Terre Environnement, INRS, 490 De la Couronne Street, Québec City, QC G1K 9A9, Canada;
karem.chokmani@inrs.ca

* Correspondence: ridha.guebsi@inrs.ca

Abstract

This study investigates the effects of key atmospheric features on mineral dust emissions and transport in the Sahara–Sahel region, focusing on the Bodélé Depression, during June 2006 and 2011. We use a combination of high-resolution atmospheric simulations (AROME model), satellite observations (MODIS), and reanalysis data (ERA5, ECMWF) to examine the roles of the low-level jet (LLJ), Saharan heat low (SHL), Intertropical Discontinuity (ITD), and African Easterly Jet (AEJ) in modulating dust activity. Our results reveal significant interannual variability in aerosol optical depth (AOD) between the two periods, with a marked decrease in June 2011 compared to June 2006. The LLJ emerges as a dominant factor in dust uplift over Bodélé, with its intensity strongly influenced by local topography, particularly the Tibesti Massif. The position and intensity of the SHL also play crucial roles, affecting the configuration of monsoon flow and Harmattan winds. Analysis of wind patterns shows a strong negative correlation between AOD and meridional wind in the Bodélé region, while zonal wind analysis emphasizes the importance of the AEJ and Tropical Easterly Jet (TEJ) in dust transport. Surprisingly, we observe no significant correlation between ITD position and AOD measurements, highlighting the complexity of dust emission processes. This study is the first to combine climatological context and case studies to demonstrate the effects of African monsoon variability on dust uplift at intra-seasonal timescales, associated with the modulation of ITD latitude position, SHL, LLJ, and AEJ. Our findings contribute to understanding the complex relationships between large-scale atmospheric features and dust dynamics in this key source region, with implications for improving dust forecasting and climate modeling efforts.

Keywords: aerosol optical depth; Saharan heat low; intertropical discontinuity; African easterly jet; Bodélé; climate change



Academic Editor: Dimitris Kaskaoutis

Received: 26 May 2025

Revised: 17 July 2025

Accepted: 31 July 2025

Published: 2 August 2025

Citation: Guebsi, R.; Chokmani, K. Effects of Large- and Meso-Scale Circulation on Uprising Dust over Bodélé in June 2006 and June 2011.

Remote Sens. **2025**, *17*, 2674. <https://doi.org/10.3390/rs17152674>

Copyright: © 2025 by the authors. Licensee MDPI, Basel, Switzerland. This article is an open access article distributed under the terms and conditions of the Creative Commons Attribution (CC BY) license (<https://creativecommons.org/licenses/by/4.0/>).

1. Introduction

The Bodélé Depression, located in northern Chad (centered at 18°E, 16°N), is recognized as the world's most prolific source of atmospheric dust, contributing approximately 50% of the Sahara's total mineral dust emissions [1]. This region, the lowest point in Chad at 155 m above sea level, is a remnant of the prehistoric Mega-Chad lake, which once extended over 500 km from north to south and 150 km from east to west [2]. The sedimentary deposits within the Bodélé Depression, characterized by their abundance of diatomites, serve as a primary source of wind-driven dust emissions [3]. Over millennia, aeolian erosion has resulted in significant sediment loss, with deflation rates estimated at 1.6 mm per year, although localized erosion may exceed 10 mm annually. The mineral dust

emitted from this region exerts a critical influence on climate regulation, ocean fertilization, and atmospheric radiative forcing [4].

Numerous studies have investigated the relationship between large-scale atmospheric circulation and Saharan dust emissions. For example, [5,6] highlighted the critical role of the Bodélé low-level Jet (LLJ) in dust uplift, while [7,8] explored how the Saharan heat low (SHL) modulates regional wind patterns and dust emission. The African Easterly Jet (AEJ) has also been shown to influence dust transport pathways across West Africa [7]. Recent reviews [4,9,10] emphasize the complexity of interactions between the SHL, LLJ, AEJ, and ITD in shaping the spatial and temporal variability of dust emissions. However, most previous work has focused on seasonal or interannual averages, and few studies have systematically compared contrasting years to elucidate the mechanisms behind interannual variability at the intra-seasonal scale, which, therefore, remains poorly understood [3].

One of the key atmospheric mechanisms governing dust emissions in Bodélé is the low-level jet (LLJ), a near-surface wind system that accelerates between the Tibesti and Ennedi Massifs. The Tibesti Mountains, the highest range in the Sahara (reaching elevations above 3000 m), extend across northern Chad and southern Libya. The Ennedi Massif, a sandstone plateau, rises to 1450 m and spans 40,000 km². The LLJ exhibits heightened activity from October to March, driving intense wind erosion and dust uplift [11]. Additionally, several large-scale atmospheric features, including the Saharan heat low (SHL), the Intertropical Discontinuity (ITD), and the African Easterly Jet (AEJ), influence the transport and variability of dust emissions.

The choice of June 2006 and June 2011 is not arbitrary. These two years correspond to major international field campaigns, AMMA (African Monsoon Multidisciplinary Analysis) in 2006 and Fennec (an international field campaign focused on the central Sahara) in 2011, which provided unprecedented observational coverage of the Saharan region. This allows for robust validation of model outputs and a unique opportunity to investigate atmospheric processes during periods with well-documented meteorological conditions and dust events [12,13].

The study first examines the dominant circulation patterns affecting dust emissions, including SHL, LLJ, ITD, and AOD variability. We then analyze the key differences between June 2006 and June 2011, focusing on the factors responsible for variations in dust uplift and transport. Finally, we assess the role of atmospheric circulation anomalies in explaining the observed differences in AOD. Overall, this study provides new insights into the mechanisms linking regional atmospheric circulation and dust emissions over Bodélé and demonstrates the value of combining climatological context with case-specific analysis. These results have important implications for improving dust forecasting and understanding climate feedback in the Sahara–Sahel region.

2. Materials and Methods

2.1. Study Area and Periods

The Bodélé Depression has long been recognized as one of the world's primary dust sources [14–17]. Recent studies have solidified its status as the most intense dust source globally, contributing about 50% of mineral dust emissions from the Sahara [18] (Figure 1).

Our study focuses on two key regions: the Saharan heat low (SHL) area (5°W–10°E, 16°N–20°N) and the Bodélé Depression (5°E–20°E, 16°N–20°N) (Figure 2). By comparing these two regions, we aim to better characterize the specific climatic and topographic factors that control dust uplift and transport in the central Sahara [10].

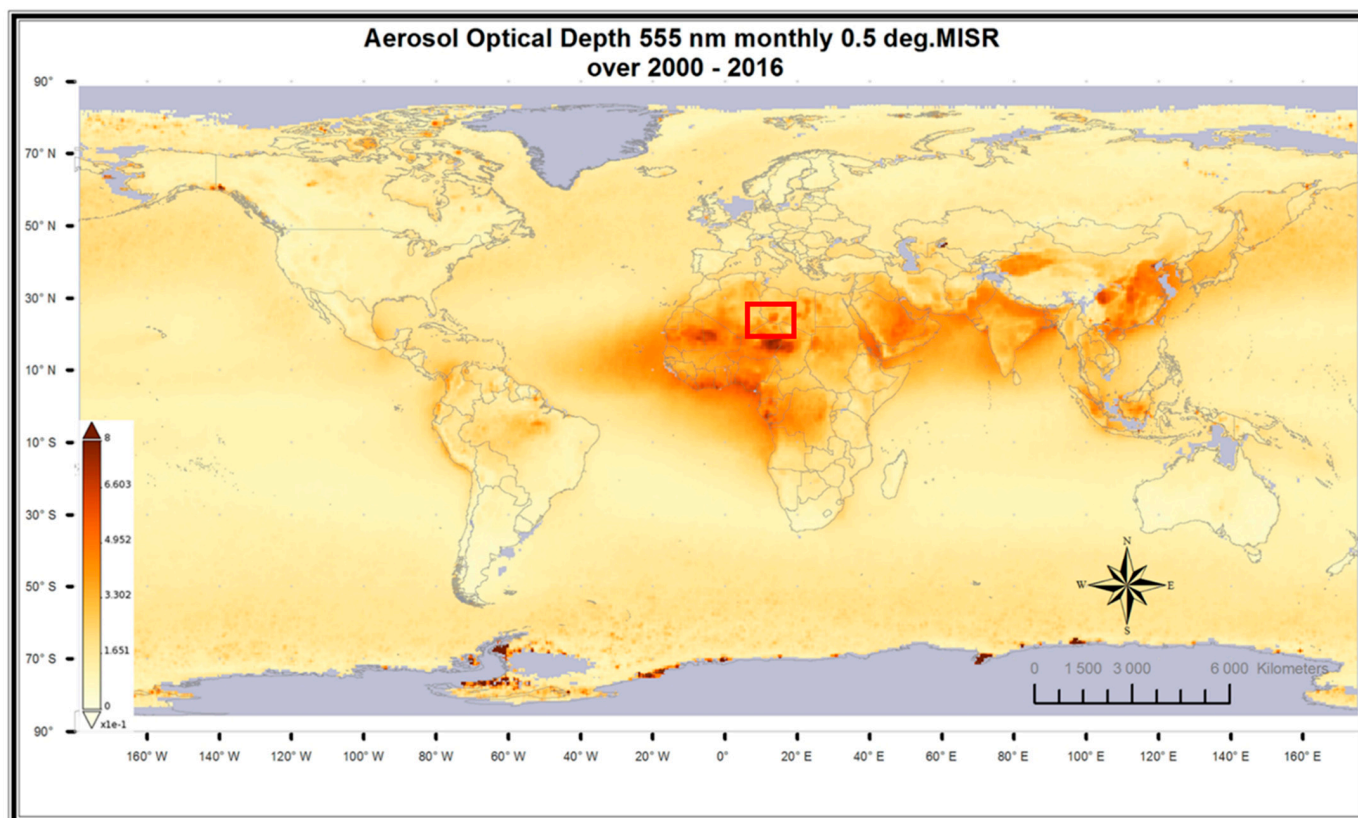


Figure 1. Global scale mean of aerosol optical depth (AOD) from 2000 to 2016 based on observations from a Multi-angle Imaging Spectroradiometer (MISR) at 555 nm. AOD measures how aerosols in the atmosphere affect the transmission of sunlight. Values below 0.1 (represented by pale yellow) indicate clear skies with high visibility, while values of 1 (shown in reddish brown) signify very hazy conditions. The red square highlights the maximum AOD recorded in the Bodélé region, reflecting a significant concentration of aerosols in that area.

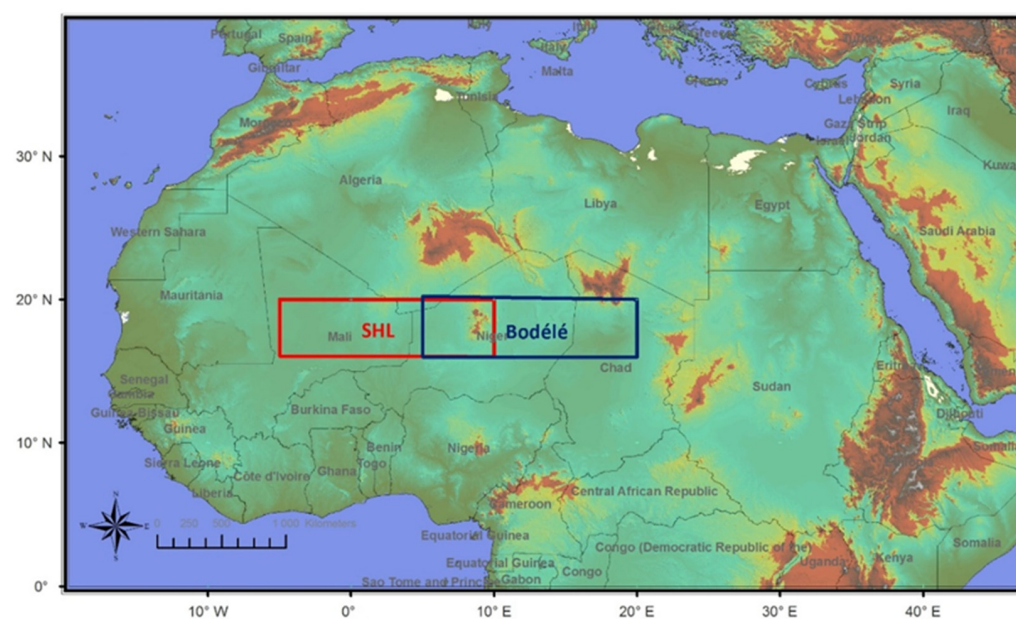


Figure 2. Red: Saharan heat low, SHL region (5°W, 10°E, 16°N, 20°N); blue: Bodélé region (5°E, 20°E, 16°N, 20°N).

A key atmospheric feature in this region is the Bodélé low-level jet (LLJ), embedded within the northeasterly Harmattan winds, which are characteristic trade winds over West Africa from November to March [7]. The LLJ plays a crucial role in focusing on erodible sediments, driving dust emission and transport. The regional topography, particularly the Tibesti and Ennedi Mountains, significantly accelerates near-surface flow [19].

Our study benefits from the comprehensive datasets provided by two major field campaigns: the AMMA in 2006 and the Fennec project in 2011. These campaigns, complemented by satellite observations and model assimilations, offer invaluable insights into the atmospheric characteristics of the Bodélé region [8,20].

Recent research has highlighted the long-term interplay between topography, wind patterns, and dust emissions in maintaining this significant dust source over geological time scales [3].

2.2. Data Collection

Our study of atmospheric dust over the Bodélé Depression and Saharan heat low region integrates data from multiple satellite platforms, high-resolution model simulations, and ground-based measurements. This comprehensive approach enables a thorough analysis of dust dynamics in these critical regions.

Satellite observations form a cornerstone of our data collection. We utilized the Multi-angle Imaging Spectroradiometer (MISR) and Moderate Resolution Imaging Spectroradiometer (MODIS) instruments aboard the Terra satellite (EOS AM-1, NASA, 1999-068A). Specifically, MISR and MODIS Level-1B data from channels 4, 3, and 1, which were obtained for June 2006 and June 2011, were employed to construct a climatology of dust plume frequency over our region of interest. These instruments provide crucial information on aerosol optical properties and dust distribution patterns.

To complement satellite observations, we employed high-resolution simulations from the AROME (Applications of Research to Operations at Mesoscale) model [21,22]. AROME has demonstrated a robust capability for reproducing the dust life cycle [23], showing strong agreement with AERONET station observations and Deep Blue daily mean aerosol optical depth (AOD) measurements [24].

For large-scale atmospheric circulation data, we used the ERA5 reanalysis from ECMWF (the European Centre for Medium-Range Weather Forecasts), which provides hourly data at a $0.25^\circ \times 0.25^\circ$ spatial resolution [25]. ERA5 offers improved accuracy in representing the Saharan heat low (SHL), low-level jets, and other key features, and was used consistently throughout this study for all atmospheric analyses [7].

While MODIS and MISR provide robust estimates of total aerosol optical depth (AOD), they do not distinguish between dust and other aerosol types. This limitation is acknowledged, and future work should consider dust-specific satellite products, such as MIDAS.

Model outputs from AROME were validated against MODIS and MISR satellite observations and AERONET ground-based measurements, ensuring the robustness of simulated AOD and wind fields.

Our analysis is further enriched by the incorporation of the Modern-Era Retrospective analysis for Research and Applications version 2 (MERRA-2). This NASA atmospheric reanalysis provides valuable insights into aerosol processes and their interactions with climate [26] using the Goddard Earth Observing System Model, Version 5 (GEOS-5), with its Atmospheric Data Assimilation System (ADAS), version 5.12.4 [26,27].

To validate our model results and satellite observations, we utilized ground-based measurements from the Aerosol Robotic Network (AERONET) [28]. AERONET provides high-quality, multi-wavelength aerosol optical depth measurements, which serve as crucial ground-truth information for our satellite and model-derived data.

This multi-faceted approach, integrating satellite observations, model simulations, and ground-based measurements, enables a comprehensive and robust analysis of dust dynamics in the Bodélé Depression and Saharan heat low region. By leveraging these diverse data sources, we aim to provide a nuanced understanding of the complex atmospheric processes governing dust emission and transport in these critical areas.

2.3. Methodology

2.3.1. Definition of Key Atmospheric Features

The Saharan heat low (SHL) was defined as the maximum low-level atmospheric thickness (LLAT, geopotential height difference between 700 and 925 hPa), computed from ERA5 data, following [7,25].

The Intertropical Discontinuity (ITD) was identified as the latitude of the maximum gradient in 925-hPa relative humidity and wind direction, marking the boundary between the Harmattan and monsoon flows, after [5].

The Bodélé low-level jet (LLJ) was defined as the daily maximum wind speed at 925 hPa between the Tibesti and Ennedi massifs (18°N–19°E), according to [3] and as resolved in ERA5 and AROME model outputs.

The African Easterly Jet (AEJ) was defined as a wind maximum in the 600–700 hPa layer, following [5,29].

2.3.2. Analysis of Atmospheric Circulation Features

The role of key atmospheric features in modulating dust uplift and transport over the Bodélé Depression was investigated. The Saharan heat low (SHL), a prominent thermal low-pressure system over the Sahara, was analyzed to assess its seasonal and interannual variability using ERA5 reanalysis data. The Intertropical Discontinuity (ITD), representing the boundary between the dry, dusty Harmattan winds and the moist monsoonal flow, was tracked using gradients in relative humidity and wind direction. Wind speed and direction at multiple pressure levels (e.g., 925 hPa for low-level jets and 700 hPa for mid-level jets) from both ERA5 and AROME were analyzed to assess the impact of the Bodélé low-level jet (LLJ), African Easterly Jet (AEJ), and Tropical Easterly Jet (TEJ) on dust transport pathways.

2.3.3. AOD Variability and Dust Source Activation

Aerosol optical depth (AOD) values derived from MODIS and MISR satellite observations were used to examine dust concentrations and variability during June 2006 and June 2011. To gain a deeper understanding of dust source activation, AOD anomalies were compared with surface wind fields from both ERA5 and AROME, as well as SHL intensity.

The AROME model was integrated to simulate atmospheric conditions and dust transport (including vertical distribution) for both months. Model outputs were evaluated against MODIS Aqua (12:00 UTC) and MODIS Terra (08:55 UTC) data, providing complementary perspectives for the daily cycle. High-resolution simulations using AROME, combined with a dust module for West Africa, were employed to calculate diurnal and nocturnal AOD variability. The methodology enabled a detailed examination of temporal and vertical variations in dust, overcoming some satellite retrieval limitations.

A case study approach was employed to investigate the interactions between dust emissions in the Bodélé Depression and the larger-scale Saharan heat low region, aiming to identify the climatic factors driving the differences in AOD and dust activity between the two years.

In summary, the methodology began by comparing the Bodélé Depression with the Saharan heat low (SHL) region to identify the unique characteristics of the Bodélé region. The study then focused on examining the significant differences in AOD between June 2006 and June 2011, followed by an analysis of key atmospheric variables, such as the

Intertropical Discontinuity (ITD), SHL, and low-level jet (LLJ). Statistical analyses, including graphical comparisons and the evaluation of difference values, were used to assess the relationships between AOD and these meteorological variables. This approach provided insights into the climatic factors driving dust emissions and transport, enabling a deeper understanding of the temporal and vertical variability in dust activity. The comprehensive analysis allowed for a better understanding of dust dynamics in the Bodélé Depression and its connection to broader atmospheric systems.

3. Results

Our analysis of AROME simulations and MODIS observations reveals significant interannual variability in dust activity over the Bodélé Depression between June 2006 and June 2011. Simulated aerosol optical depth (AOD) shows a clear decrease in 2011, and a pronounced diurnal cycle (amplitude up to 0.2) not fully detected by MODIS due to temporal sampling limits.

3.1. Analysis of Key Atmospheric Features

This section presents an analysis of the key atmospheric features influencing dust emissions and transport in the Bodélé Depression during June 2006 and June 2011. These features include aerosol optical depth (AOD), the low-level jet (LLJ), the Saharan heat low (SHL), and the Intertropical Discontinuity (ITD).

3.1.1. Aerosol Optical Depth (AOD) in June 2006 and June 2011

To illustrate the variability of aerosol optical depth (AOD) for June 2006 and 2011, Figure 3 presents the average meridional profile (from 16°E to 20°E) of AOD, derived from simulations using the AROME (Applications of Research to Operations at Mesoscale) model. As shown in Figure 3, the vertical distribution of aerosols in June 2006 extended up to 600 hPa, whereas in June 2011, dust layers remained mostly below 800 hPa.

Figure 4c compares the AOD distributions for June 2011 (Figure 4b) and June 2006 (Figure 4a) from both MODIS and AROME. Both datasets confirm a marked decrease in AOD in 2011 relative to 2006. The diurnal cycle of simulated AOD reached 0.2 in amplitude (Figure 5), demonstrating intra-day variability that is not captured by MODIS Deep Blue data due to sparse temporal coverage [23].

Recent studies have highlighted the importance of high-resolution modeling in capturing the complex dynamics of dust emissions in the Sahara. For example, [30] emphasized the role of nocturnal low-level jets in dust emission, processes that are often inadequately represented in global models.

The maximum AOD value observed in June 2006 was approximately 1, with a monthly average of 0.6 (Figure 5). In contrast, the monthly average AOD for June 2011 was 0.4, indicating weaker dust loading over the Bodélé region. Despite this decrease, the dust loading remained significant, highlighting substantial interannual variability. This variability aligns with the findings of [29], who linked year-to-year variations in North African dust emissions to large-scale atmospheric conditions.

To understand the drivers behind the substantial difference in AOD between the two years, an analysis of the climatic features of the Saharan region at both regional and large scales is essential. The authors of [9] emphasized the importance of considering synoptic-scale atmospheric patterns in conjunction with local topography when analyzing dust emission variability.

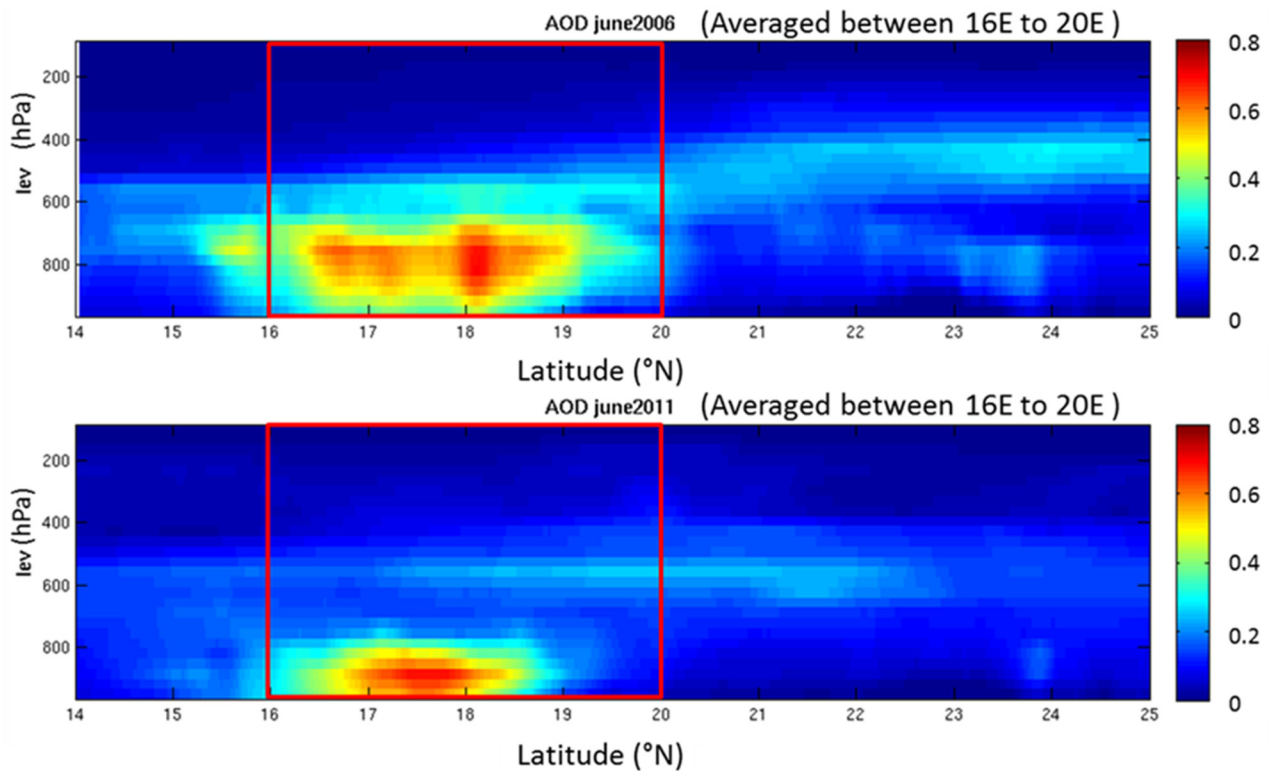


Figure 3. Comparison between June 2006 and June 2011 of vertical distributions of aerosols by latitude, averaged between 16°E and 20°E (Bodélé region) and derived from simulations using the AROME model; Red squares represent the atmosphere of Bodélé between 16°N and 20°N, averaged between 16°E and 20°E.

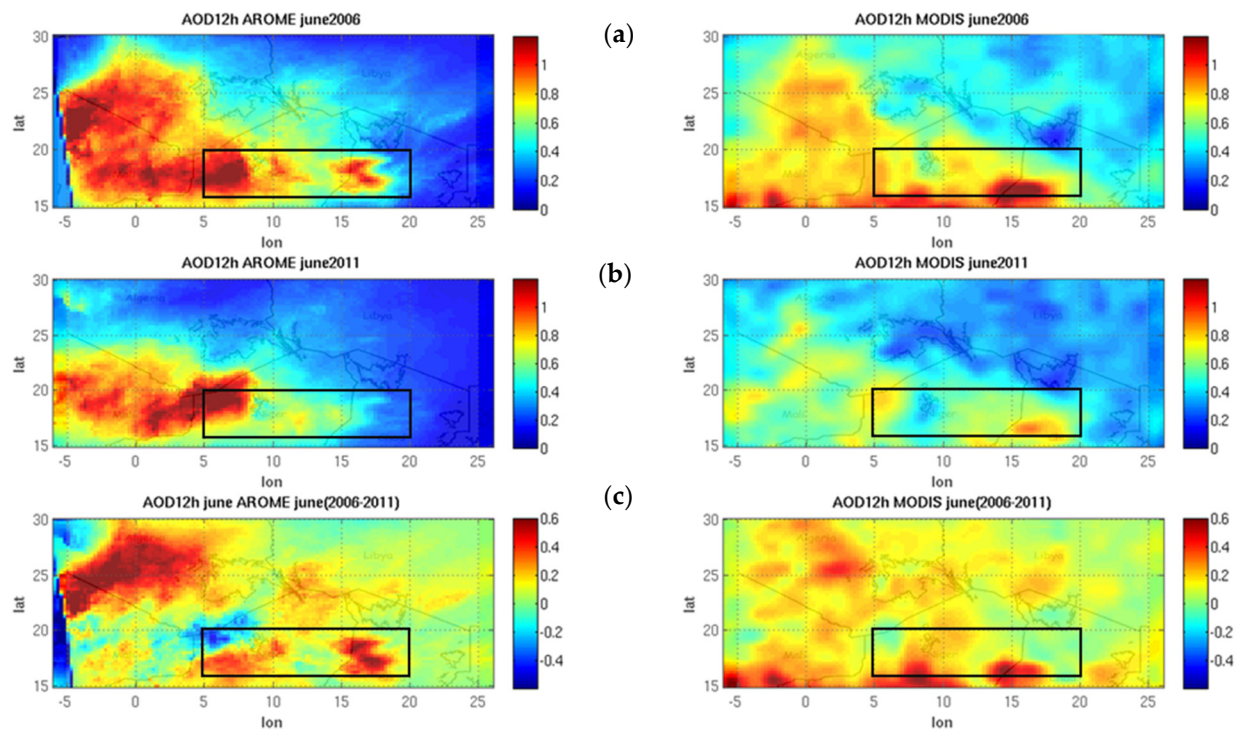


Figure 4. Comparison between June 2006 (a) and June 2011 (b) of the distribution of aerosols that is derived from the simulation AROME model on the right and MODIS observations on the left. AOD June 2006 minus AOD June 2011 (c) over Bodélé (the black box).

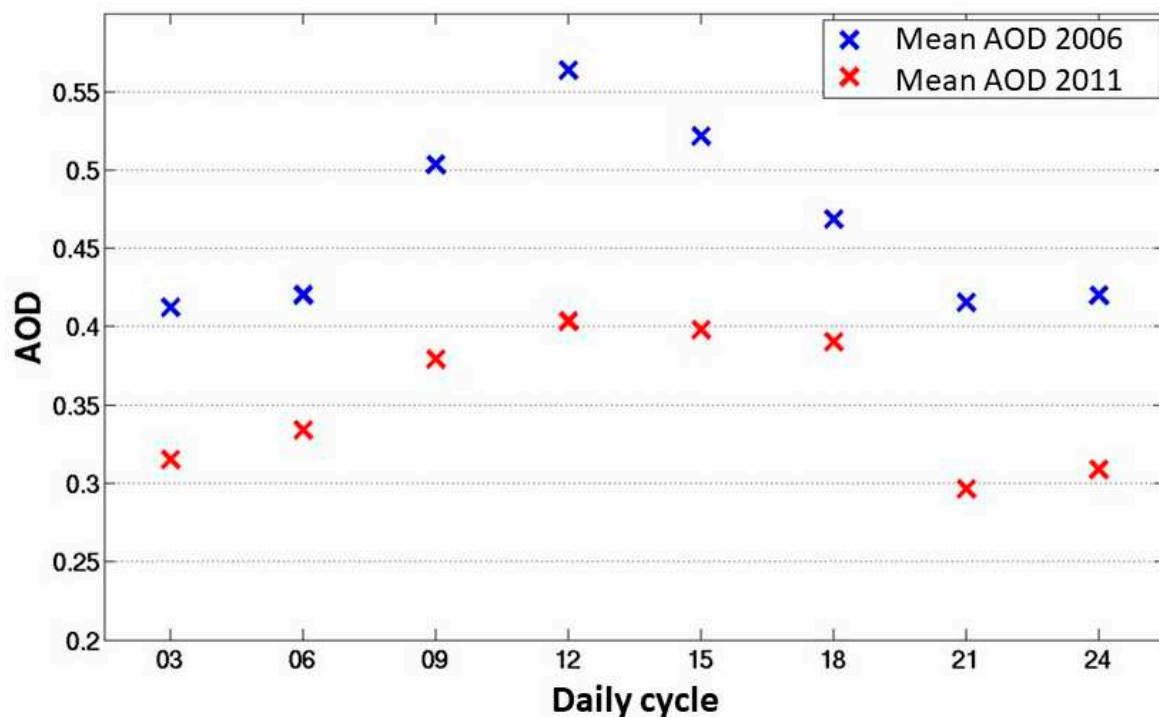


Figure 5. Diurnal AOD simulated by AROME for June 2006 and June 2011. Maximum value at 12 UTC for the two seasons. UTC: Coordinated Universal Time (formerly GMT).

The diurnal variability simulated by AROME shows peak mean AOD values for both June 2006 and June 2011 occurring at 12:00 UTC (Coordinated Universal Time), as shown in Figure 5. A clear diurnal decrease in AOD values was observed in 2011. This pattern aligns with recent studies highlighting the significance of diurnal variations in dust emissions and transport in the Sahara region [12,31].

In summary, June 2006 was characterized by both higher AOD and greater vertical dust transport than June 2011, as consistently shown by both model simulations and satellite observations.

3.1.2. Low-Level Jet (LLJ)

A key feature of the atmospheric circulation in the Bodélé Depression region is the low-level jet (LLJ), characterized by a maximum in low-level easterly winds. Recent high-resolution reanalysis data (ERA5) have enhanced our understanding of this phenomenon [25].

The LLJ typically exhibits wind speeds approaching 10 m s^{-1} at approximately 925 hPa near 18°N and 19°E (Figure 6). This feature is most pronounced during winter months, coinciding with peak dust emissions in the Bodélé Depression [7]. The jet core is typically located between 900 and 925 hPa, slightly lower in the atmosphere than previously suggested based on ERA5 data [18].

LLJ formation and intensity are closely linked to the region's unique topography. The jet aligns with the exit gap of northeasterlies between the Tibesti Mountains (2600 m) and the Ennedi Massif (1000 m), which channel and accelerate flow over the Djourab Desert in Chad [9,32]. This topographic influence creates a 'split' in the low-level easterly flow, concentrating wind energy in the Bodélé region.

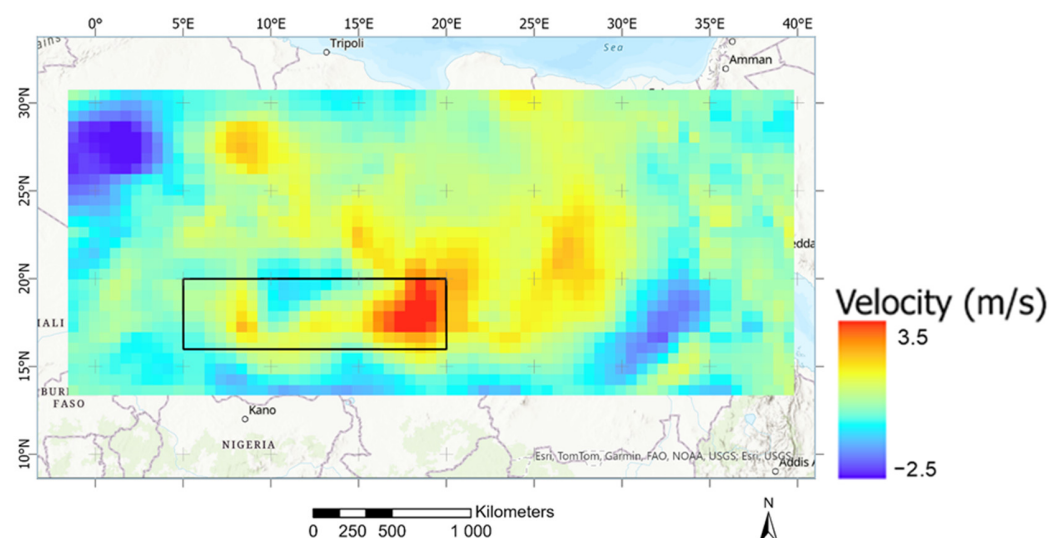


Figure 6. Surface wind speed difference between June 2006 and June 2011.

While the persistent position and core intensity of the Bodélé low-level jet (LLJ) are set by the channeling of the Harmattan winds between the Tibesti and Ennedi massifs, our analysis indicates that interannual LLJ variability is mainly controlled by regional atmospheric circulation, specifically, shifts in the Saharan heat low (SHL) and monsoon progression, and can be further modulated by upper-level jets (e.g., the African Easterly Jet, AEJ) and remotely by sea surface temperature (SST) anomalies linked to the El Niño–Southern Oscillation (ENSO).

The LLJ is a distinctive feature of the Bodélé area and is absent at other longitudes along 18°N in West Africa. This specificity is crucial for understanding the region’s role as a major global dust source [5].

The jet exhibits a marked seasonal cycle that is closely associated with dust activity. It is most active from October to March and relatively inactive ($<3 \text{ m s}^{-1}$) from June to August [33]. This seasonality is linked to large-scale atmospheric circulation patterns and local thermal gradients.

Figure 6 illustrates wind speed differences between June 2006 and 2011 over the Bodélé region. Negative values indicate wind slowdown in 2006, with high values observed between the Tibesti and Ennedi Mountains. This interannual variability in LLJ strength has a considerable impact on dust emission rates and transport patterns [1,34].

Ref. [35] suggests that climate change may alter LLJ intensity and seasonality, potentially changing dust emission patterns in this critical region.

Continued high-resolution modeling and observational studies are essential to better understand and predict these changes and their implications for global dust transport and climate feedback.

3.1.3. Saharan Heat Low (SHL)

The Saharan heat low (SHL) is a key feature of the West African climate system, playing a crucial role in the African monsoon dynamics. Recent high-resolution reanalysis data (ERA5) have significantly improved our understanding of SHL structure and variability [7,34].

The intensity of potential temperatures and the position of the SHL’s center of gravity (Figure 7) are now more accurately simulated using advanced ECMWF reanalysis techniques. These improved estimates enhance the realism of SHL simulations, which is critical for understanding its influence on the African Monsoon [36].

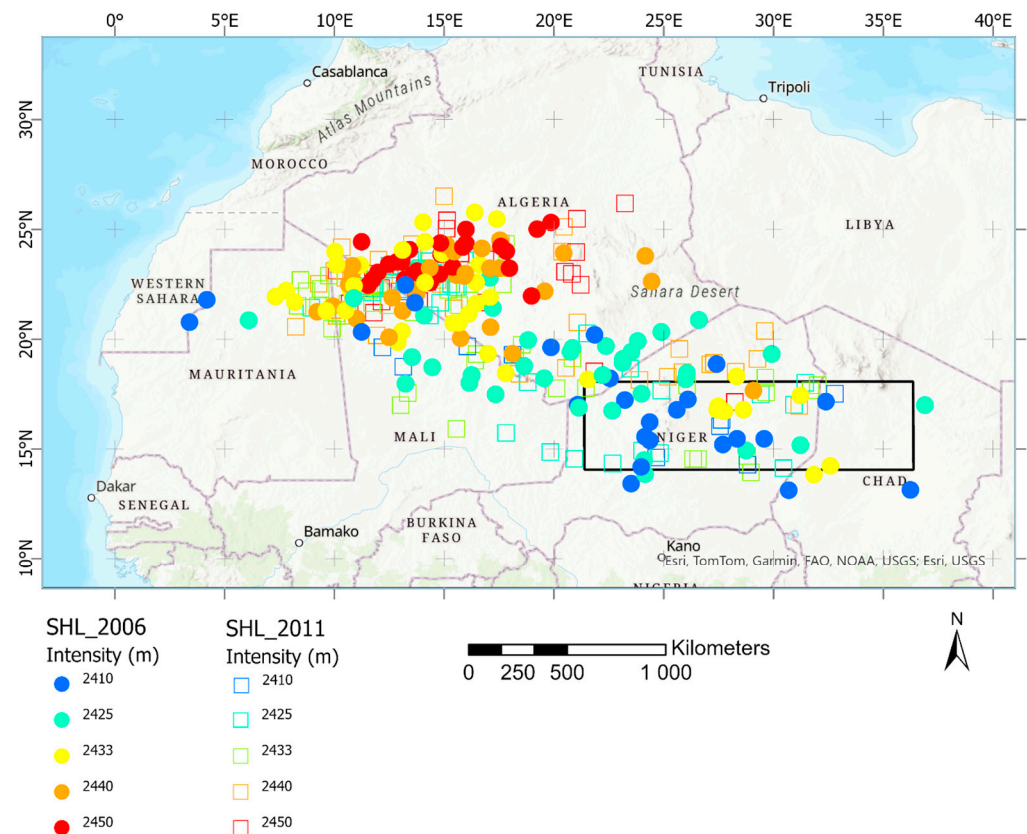


Figure 7. Position of Saharan heat low from May to September season of 2006 (closed circles) and 2011 (open squares). The color gradient indicates the intensity of the Saharan heat low, measured by the Low-Level Atmospheric Thickness (LLAT) in meters.

In June 2006, the SHL was less intense and reached a more southerly position compared to June 2011. Conversely, in June 2011, the SHL shifted to the southeastern Hoggar region (southern Algeria), exhibiting a northwestern anomaly relative to climatology. This interannual variability in SHL dynamics significantly impacts the configuration of monsoon flow and Harmattan winds.

Ref. [37] highlighted the SHL's role in modulating dust emissions and transport across the Sahara. The SHL's intensity and position have been linked to variations in dust uplift potential and transport pathways, emphasizing its importance in regional climate dynamics [38].

3.1.4. Intertropical Discontinuity Zone (ITD)

The Intertropical Discontinuity (ITD), also known as the Intertropical Front (ITF) or Intertropical Convergence Zone (ICZ), is a near-surface boundary dividing Africa into two distinct climatic zones from the Atlantic to Sudan [39]. South of the ITD, the monsoon flow contains high energy and extends to about 800–850 hPa. North of the ITD, a very dry northerly flow that is characterized by low dew-point values prevails.

Ref. [40] refined the criteria for identifying and tracking the ITD. To delineate the ITD, one of three main criteria is typically used:

- Surface convergence line at a height of 10 m (or 950 hPa) between southwest and northeast winds, particularly applicable at night.
- Sharp gradients in surface moisture, often based on relative humidity contours around 40%.

- c. The minimum pressure line, which is particularly useful near West Africa's coast where other criteria are difficult to apply. This criterion is well-suited for the thermal depression in northern Mali and Mauritania, which lie close to the ITD.

In this study, we delineated the ITD position using relative humidity fields, following recent methodologies that have proven effective for ITD identification and tracking [41]. Among the various criteria proposed in the literature, such as surface convergence, minimum pressure, or sharp gradients in relative humidity, we selected the 40% relative humidity contour as the main threshold, which has shown improved accuracy in previous works. This approach is illustrated in Figure 8a,b for June 2006 and June 2011, respectively, and the extracted ITD positions are presented in Figure 8c.

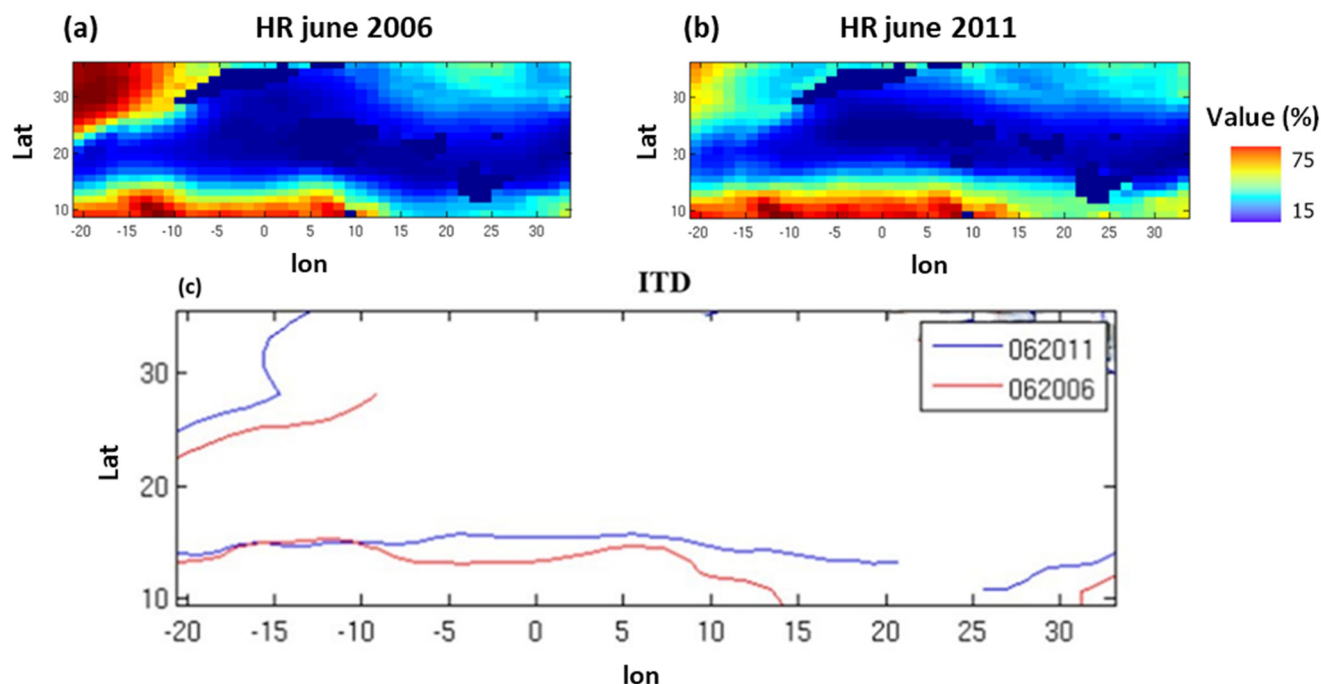


Figure 8. Relative humidity over the Saharan region for June 2006 (a) and June 2011 (b) and the Intertropical Discontinuity (ITD) extracted from relative humidity (RH = 40%) for the two periods (red: June 2006; blue: June 2011) (c).

The ITD's position and movement have been increasingly recognized as critical factors in dust emission and transport processes in the Sahel and southern Sahara [8]. Its northward progression during the monsoon season influences the timing and intensity of dust events, highlighting the complex interactions between large-scale atmospheric features and dust dynamics in the region [5].

3.2. Relationship Between AOD and Key Climatic Features

This study presents a comprehensive analysis of the impact of African Monsoon variability on dust uplift, examining the modulation effects of the Intertropical Discontinuity (ITD) latitude position, Saharan heat low (SHL), low-level jet (LLJ), and African Easterly Jet (AEJ) on intra-seasonal timescales.

3.2.1. AOD and ITD Correlation

The analysis of the daily average latitude position of the ITD and the corresponding daily average aerosol optical depth (AOD) values over the Saharan heat low (SHL) and Bodélé Depression regions reveals an unexpected outcome. In June 2011, the ITD shifted notably northward, reaching around 15°N, compared to June 2006, where it remained to

the south of 14°N (Figure 8). This northward displacement of the ITD was anticipated to have a significant impact on dust emissions, potentially leading to reduced uplift in the Bodélé Depression due to a weakened low-level jet (LLJ), driven by altered pressure gradients and wind shear over the Tibesti Massif. However, contrary to these expectations, statistical analysis did not reveal a significant correlation between the ITD position and the daily AOD measurements over either the SHL (Figure 9a) or Bodélé Depression regions (Figure 9b).

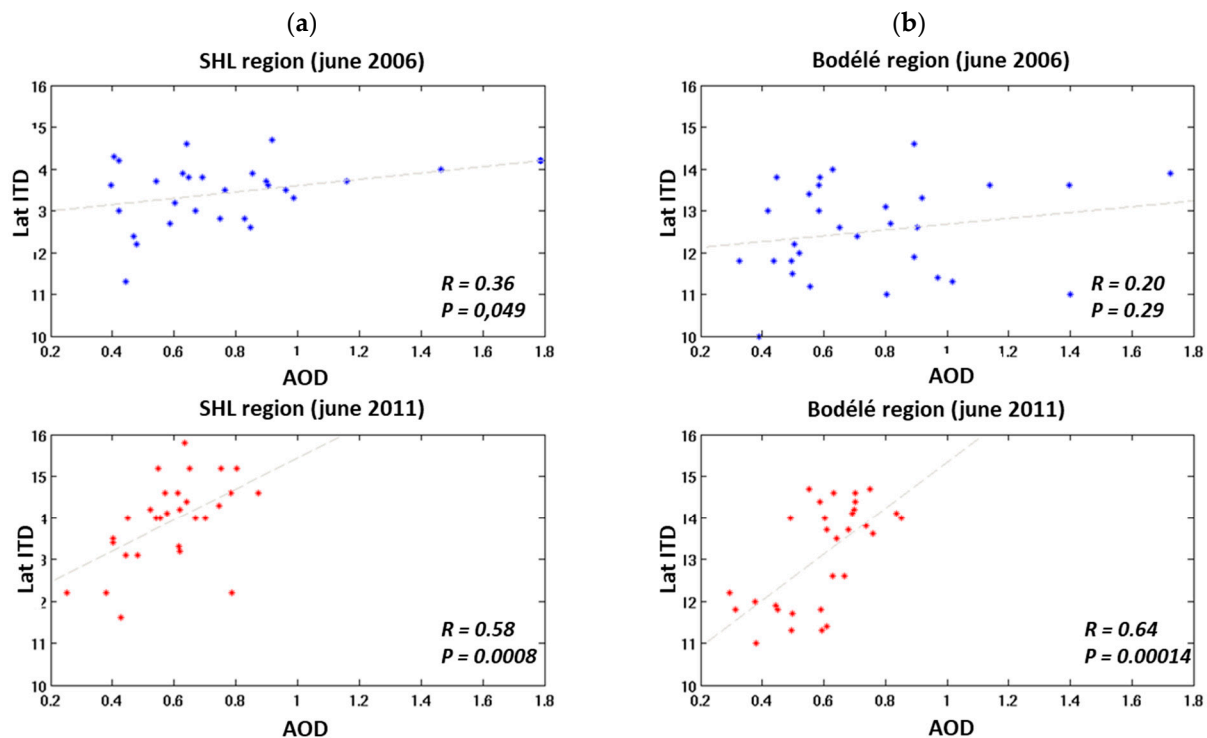


Figure 9. AOD and latitude position of ITD over SHL (5°W, 10°E, 16°N, 20°N) (a) and Bodélé (5°E, 20°E, 16°N, 20°N) (b) regions in June 2006 (blue) and June 2011 (red).

Despite the expected influence of the ITD, the analysis did not show a clear relationship between the northernmost positions of the ITD and peak AOD values.

In fact, while the ITD shifted northward in June 2011, the AOD over the Bodélé Depression was notably lower compared to June 2006, which saw stronger dust emissions and higher AOD values. This discrepancy suggests that factors other than the position of the ITD may have played a more dominant role in regulating dust activity in the region. Despite the ITD reaching latitudes above 16°N in 2011, the mean AOD values ($AOD < 0.5$) did not coincide with the northernmost positions of the ITD, highlighting the complexity of the relationship between the ITD and dust emissions (Figure 9).

These results align with previous studies that have emphasized the complex and often non-linear relationship between the ITD and dust emissions in the Sahara. The absence of a significant correlation suggests that other atmospheric and environmental factors, such as surface wind speeds, atmospheric stability, and soil moisture conditions, may exert a more direct influence on dust emission variability, especially on shorter time scales. These findings emphasize the need for further investigation into the roles of these additional drivers in order to better understand the factors that modulate dust emissions in the Bodélé Depression and the wider Saharan region [5].

3.2.2. AOD in Relation to SHL Position and Intensity

Analysis of the Saharan heat low (SHL) reveals significant interannual variability in both its position and intensity. In June 2006, the SHL exhibited an unusually southerly position, with its center of gravity reaching 18°N during the first half of the month, particularly in its eastern sector. This represents a displacement of approximately 2° latitude south of the 30-year climatological mean (1980–2012) for June (Figure 10), potentially influencing regional wind patterns and dust source activation over Bodélé.

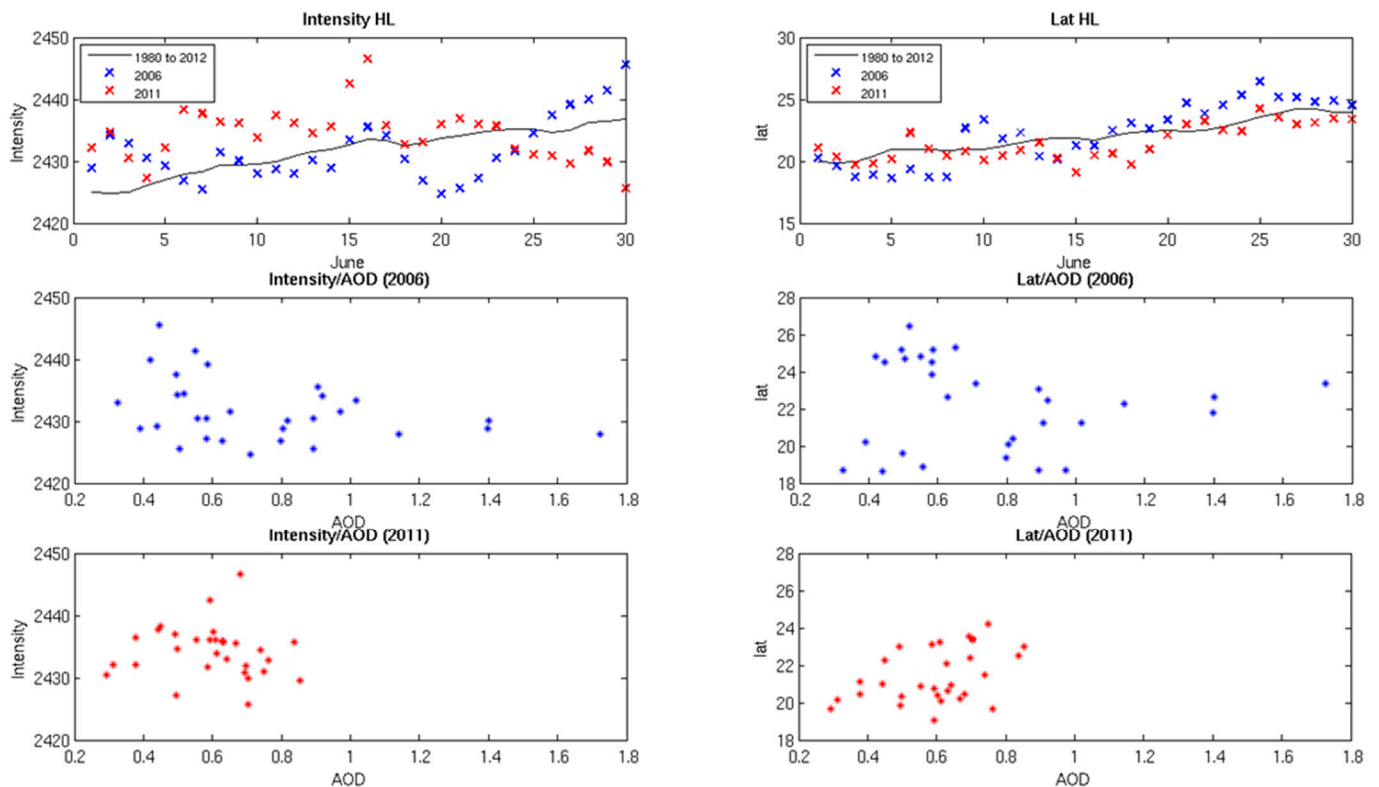


Figure 10. AOD compared with the intensity and latitude position of Saharan heat low (SHL) for June 2006 (blue) and June 2011 (red) and the seasonal (June) average from 1980 to 2012 (black line).

SHL intensity, as quantified by Low-Level Atmospheric Thickness (LLAT), was more pronounced during early June 2011 compared to June 2006. A notable intensification of the SHL was observed after 20 June 2006 over the Hoggar region, characterized by LLAT values exceeding 2440 m. However, we found no statistically significant correlation between AOD values and the latitudinal position of the SHL over the Bodélé Depression.

This lack of a direct linear relationship between SHL characteristics and AOD is consistent with previous studies [1], indicating that the SHL's influence on dust emissions is complex and indirect, potentially mediated by its modulation of regional wind patterns, atmospheric stability, and the strength of the Harmattan winds. While the SHL undoubtedly plays a significant role in shaping the regional climate system, its direct control on dust emission variability in the Bodélé Depression appears to be limited.

3.2.3. AOD and Meridional Wind Interaction

Our analysis reveals a notable interaction between AOD and meridional winds in the Bodélé Depression, with the low-level jet (LLJ) playing a significant role in dust mobilization (Figure 11a,b). AOD values during early June 2006 were almost double those of June 2011, suggesting much stronger dust source activation in 2006 compared to 2011. This difference can largely be attributed to the stronger meridional winds in 2006, which were

not restrained by the developing monsoon, as opposed to June 2011, where the monsoon had a moderating effect on the Harmattan winds, leading to reduced dust mobilization [9].

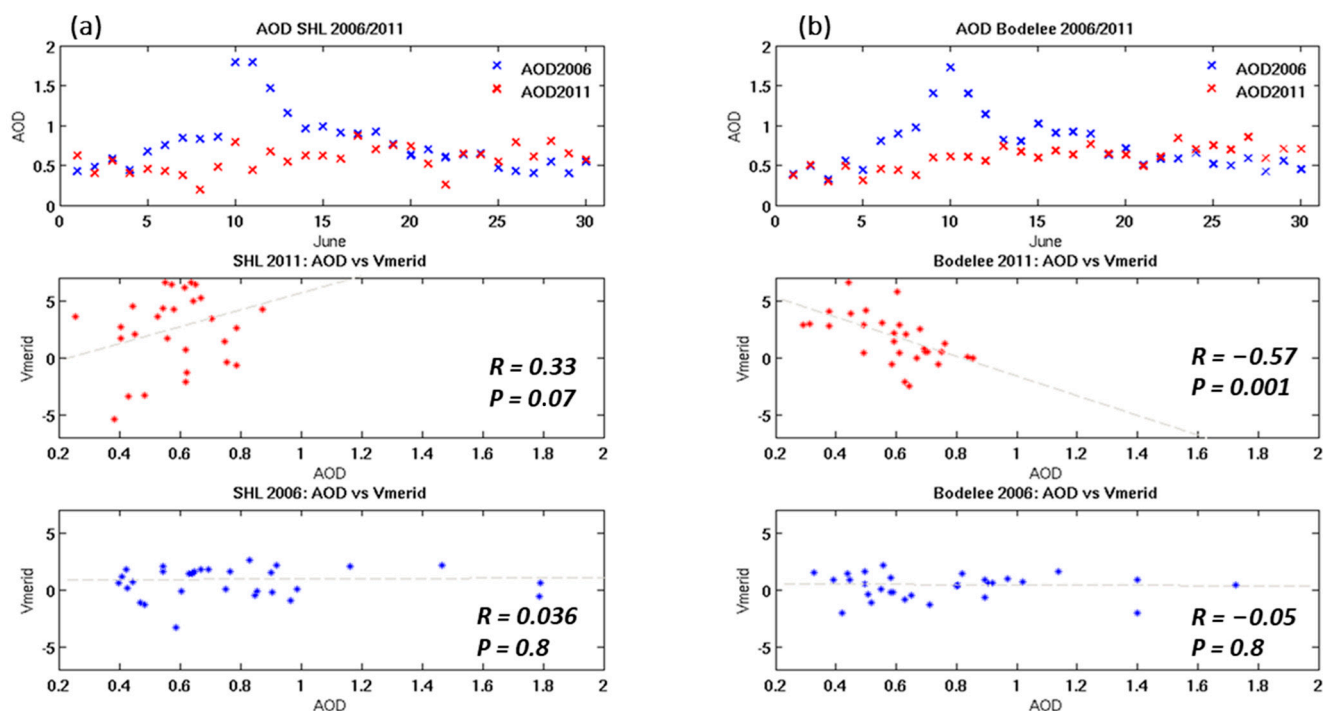


Figure 11. AOD and meridional wind (negative values indicate southward flow) over SHL (5°W, 10°E, 16°N, 20°N) (a) and Bodélé (5°E, 20°E, 16°N, 20°N) (b) regions for June 2006 (blue) and June 2011 (red).

In June 2006, the meridional winds were stronger, with southward flow (negative meridional winds) enhancing dust uplift, while in 2011, the meridional winds were weaker and even exhibited a negative correlation with AOD, particularly over the Bodélé region. The topography of the Tibesti Massif plays a crucial role in channeling and accelerating the low-level easterly flow, contributing to the formation of a pronounced LLJ over the Bodélé Depression (Figure 11b). The LLJ, in combination with the strong meridional winds, is a defining characteristic of the Bodélé region and plays a central role in its status as a globally significant dust source.

3.2.4. AOD and Zonal Wind Dynamics

Our analysis of the zonal wind patterns over the Bodélé region reveals a significant relationship between the spatial extent of the wind and the observed aerosol optical depth (AOD) during June 2006 and 2011. In June 2006, the zonal wind exhibited a broader longitudinal span from 10°E to 22°E, with sustained wind speeds averaging around 10 m/s. This extensive wind field coincided with higher AOD values, with a mean of 1.2 between 5 and 19 June 2006 (Figure 12a,b). Conversely, in June 2011, the zonal wind was confined to a narrower longitudinal range between 16°E and 22°E, with slightly lower wind speeds (10 m/s), corresponding to lower AOD values of 0.5 during the same period (Figure 12c).

This substantial increase in the longitudinal span of the zonal wind in 2006 compared to 2011 aligns with the observed higher AOD values in 2006. The broader wind field in 2006 likely facilitated the transport of dust particles over a larger area, contributing to higher dust mobilization and aerosol loading in the region. The figure illustrating this trend further supports this correlation, showing a marked increase in AOD levels during the first half of June 2006, corresponding with the broader wind zone.

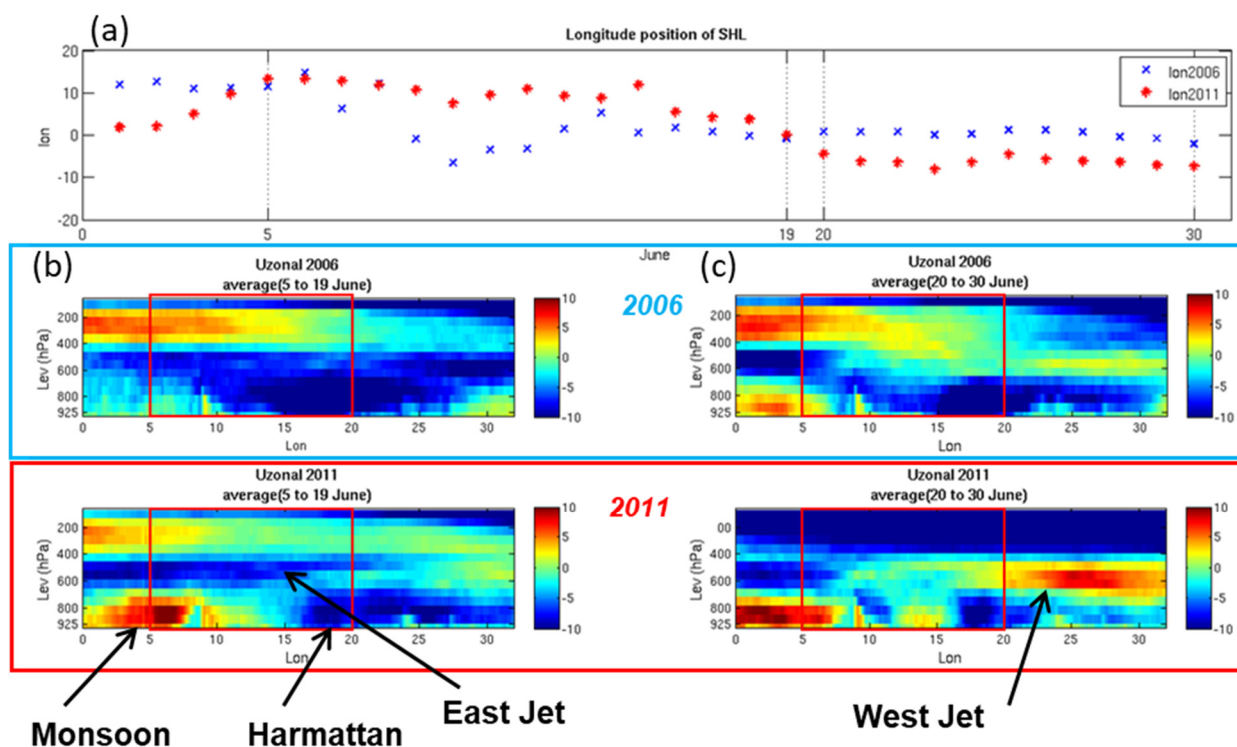


Figure 12. (a) Daily longitude position of SHL (June 2006 and June 2011); (b) uzonal average from 5 to 19 June: 2006 and 2011; (c) uzonal average from 20 to 30 June 2006 and 2011 over 18°N and from 0 to 32°E by level (hPa).

These findings suggest that the extent and intensity of the zonal wind, particularly its spatial reach across the region, play a crucial role in influencing the amount of dust uplifted and transported from the Bodélé Depression. This conclusion highlights the complex interaction between atmospheric circulation patterns and dust dynamics, underscoring the need for a deeper understanding of how wind patterns can drive interannual variability in dust emissions (Figure 12).

The enhanced AEJ activity during June 2006 likely facilitated more efficient dust transport away from the Bodélé Depression region, potentially contributing to the higher AOD values observed during this period. Conversely, the weaker AEJ and stronger TEJ in June 2011 may have resulted in a different dust transport regime, with implications for the spatial distribution of dust aerosols.

The AROME model was integrated to simulate atmospheric conditions, providing crucial insights into dust transport and vertical distribution. In June 2006, significant dust uplift was observed over the Bodélé Depression, with vertical transport reaching the 600 hPa level, while in June 2011, dust transport was confined to below 800 hPa, indicating reduced dust activity. This decrease in AOD is corroborated by both AROME simulations and MODIS measurements. To validate the AROME data, MODIS Aqua (at 12:00 UTC) and MODIS Terra (at 08:55 UTC) observations were used, offering complementary perspectives for a full 24 h daily cycle. AROME simulations reveal a pronounced diurnal cycle in AOD (amplitude up to 0.2; Figure 5), a feature not observed in MODIS Deep Blue due to limited temporal resolution. This highlights the importance of high-frequency modeling for capturing daily variability in dust emissions.

4. Discussion

Our comprehensive investigation into dust dynamics in the Bodélé Depression reveals a complex interplay between large-scale atmospheric patterns and regional topography,

resulting in significant interannual variability in aerosol optical depth (AOD) between June 2006 and June 2011. This study provides novel insights into the specific roles of key atmospheric features at intra-seasonal timescales, extending our understanding of dust emission processes in this critical region.

The marked decrease in AOD observed in June 2011 compared to June 2006 suggests a fundamental shift in dust emission and transport mechanisms. Our analysis indicates that the Intertropical Discontinuity (ITD), Saharan heat low (SHL), and low-level jet (LLJ) all played significant roles in modulating dust activity during these periods. However, the relationships between these features and AOD were often complex and non-linear, highlighting the limitations of relying on simple correlations.

Contrary to initial expectations, we found no statistically significant linear correlation between ITD latitude position and daily AOD measurements. This result underscores the complexity of dust emission processes and suggests that other factors, such as wind speed, atmospheric stability, and soil moisture content, may be more direct drivers of dust emission variability. It is also possible that time-lagged effects, where the ITD's influence on dust emissions manifests over longer timescales, could explain the lack of a strong correlation.

The SHL exhibited notable differences in intensity and position between the two years, with a more intense SHL observed in early June 2011. However, high AOD values were not consistently associated with specific SHL characteristics. This complexity points towards a more nuanced role of the SHL in dust dynamics, likely mediated through its influence on regional circulation patterns, including the LLJ, and atmospheric stability.

Our analysis reveals a strong negative correlation between AOD and meridional wind over the Bodélé region in June 2011, confirming the LLJ's critical role in dust uplift. The unique topography of the region, particularly the channeling effect of the Tibesti Massif, appears to be crucial in shaping these wind patterns and facilitating dust mobilization. Specifically, the interaction between the LLJ and the Tibesti Massif creates localized regions of enhanced wind shear and turbulence, promoting the suspension of dust particles into the atmosphere.

The zonal wind analysis highlights the importance of the African Easterly Jet (AEJ) and the Tropical Easterly Jet (TEJ) in modulating dust aerosol patterns. The observed differences in jet speeds and positions between 2006 and 2011 likely contributed to variations in dust transport pathways. A stronger AEJ, as seen in 2006, may facilitate westward dust transport, while a weaker AEJ and stronger TEJ, as observed in 2011, may result in a more localized dust plume.

Our findings align with previous research by [33], which emphasized the importance of extensive cold pools (haboobs) as significant dust sources in the region, potentially contributing up to 50% of dust production during June [8]. However, as in many studies, our study faces limitations in capturing these events due to the timing of satellite passes and the inherent challenges in modeling such phenomena. These findings underscore the complex interplay between atmospheric and surface factors in controlling dust emissions from the Bodélé Depression. They highlight the need for continued high-resolution modeling and observational studies to improve our understanding and prediction of dust emission patterns in this critical region, particularly in the context of climate change and its potential effects on dust emission dynamics [42].

To further elucidate the causative relationships between atmospheric features and dust emissions, future research should employ more sophisticated modeling techniques that incorporate detailed representations of atmospheric processes and surface conditions. Additionally, the potential influence of larger-scale atmospheric phenomena, such as Rossby waves and the Indian Monsoon, on dust dynamics in the Bodélé Depression warrants investigation.

Rossby waves, being large-scale atmospheric waves, could potentially modulate the position and intensity of the SHL, AEJ, or ITD, indirectly affecting dust emission and transport from the Bodélé Depression. Similarly, the Indian Monsoon's influence on the strength and position of the TEJ could have downstream effects on dust dynamics in North Africa. Exploring these connections could provide a more comprehensive understanding of the global atmospheric processes influencing dust activity in the Sahara–Sahel region.

In summary, our study underscores the complex interplay between large-scale atmospheric features and regional and local-scale processes in driving dust emissions in the Bodélé Depression. While the ITD, SHL, LLJ, and AEJ all play significant roles, their influence on dust activity is often non-linear and modulated by other factors.

To better understand and predict dust events in this critical region, future research should prioritize several key areas. These include utilizing dust-specific datasets to improve the accuracy and specificity of AOD measurements, employing more sophisticated modeling techniques to capture the complex interactions between atmospheric features and surface conditions, and conducting multi-year observational studies to further elucidate the mechanisms through which these atmospheric features influence dust emissions, particularly in the context of climate change. Furthermore, the potential influence of large-scale phenomena like Rossby waves and the Indian Monsoon on dust dynamics in the Sahara–Sahel region warrants investigation, and efforts should be directed towards improving the representation of haboobs and other mesoscale features in climate models.

By addressing these challenges, we can move closer to a more complete understanding of dust dynamics in the Sahara–Sahel region and improve our ability to predict dust events and their far-reaching impacts on regional and global climate systems.

5. Conclusions

This study has successfully investigated the complex interactions between atmospheric dynamics and dust emissions in the Sahara–Sahel region, focusing on the Bodélé Depression during June 2006 and June 2011, periods coinciding with the AMMA and Fennec experiments. Through a combination of airborne and satellite observations and mesoscale model simulations, we provide key insights into the roles of the low-level jet (LLJ), monsoon-related winds, and Saharan heat low (SHL) anomalies in modulating dust activity.

Our findings reveal significant interannual variability in aerosol optical depth (AOD) between the two study periods, with distinct atmospheric conditions driving dust uplift and transport. Notably, the analysis highlights a marked difference in the African Easterly Jet (AEJ) intensity, with a stronger AEJ in 2006 contributing to more intense dust uplift and westward transport. The study also underscores the complex, non-linear relationships between dust emissions and atmospheric features, exemplified by the absence of a direct correlation between the Intertropical Discontinuity (ITD) position and AOD measurements. Instead, the influence of topography, particularly the Tibesti Massif, in shaping low-level wind patterns and subsequent dust emissions, emerges as a key controlling factor.

Building upon these findings, we recommend that future research endeavors to prioritize several key areas. First, the integration of dust-specific datasets, such as the MODIS MIDAS dataset, is crucial to refining the accuracy of AOD measurements. Second, the application of sophisticated modeling techniques is essential to capture the complex interactions between atmospheric features and surface conditions. Third, interannual observational studies are needed to elucidate the mechanisms through which these atmospheric features influence dust emissions, particularly in the context of climate change. Finally, future research should explore the potential influence of other large-scale atmospheric phenomena, such as Rossby waves and the Indian Monsoon, on dust dynamics in the Sahara–Sahel

region. Understanding the teleconnections between these systems and the regional climate could provide valuable insights into dust source variability and improve our ability to predict dust events. More specifically, we encourage investigation into the easterly jet and the tropical easterly jets and how they may change our understanding of current climate change and dust emissions.

By pursuing these research directions, we can continue to refine our understanding of dust emission processes and improve our ability to predict dust events and their far-reaching impacts on regional and global climate systems. The need for more specific data will allow for more precise findings.

Author Contributions: R.G.: Conceptualization, methodology, writing—original draft, writing—review and editing. K.C.: Funding acquisition, methodology, and writing—original draft. All authors have read and agreed to the published version of the manuscript.

Funding: This research did not receive any specific grant from funding agencies in the public, commercial, or not-for-profit sectors.

Data Availability Statement: The datasets and code supporting the findings of this study are available from the corresponding author upon reasonable request.

Acknowledgments: The authors would like to thank Cyrille Flamant for helpful discussions during the early stages of this work. The authors also acknowledge Cecile Kocha and Christophe Lavaysse for providing access to certain datasets used in this study.

Conflicts of Interest: The authors declare that they have no known competing financial interests or personal relationships that could have appeared to influence the work reported in this paper.

References

1. Evan, A.T.; Fiedler, S.; Zhao, C.; Menut, L.; Schepanski, K.; Flamant, C.; Doherty, O. Derivation of an observation-based map of North African dust emission. *Aeolian Res.* **2015**, *16*, 153–162. [[CrossRef](#)]
2. Bristow, C.S.; Drake, N.; Armitage, S. Deflation in the dustiest place on Earth: The Bodele Depression, Chad. *Geomorphology* **2009**, *105*, 50–58. [[CrossRef](#)]
3. Washington, R.; Todd, M.C.; Lizcano, G.; Tegen, I.; Flamant, C.; Koren, I.; Ginoux, P.; Engelstaedter, S.; Bristow, C.S.; Zender, C.S.; et al. Links between topography, wind, deflation, lakes and dust: The case of the Bodélé Depression, Chad. *Geophys. Res. Lett.* **2006**, *33*, L09401. [[CrossRef](#)]
4. Yu, H.; Tan, Q.; Chin, M.; Remer, L.A.; Kahn, R.A.; Bian, H.; Kim, D.; Zhang, Z.; Yuan, T.; Omar, A.H.; et al. Estimates of African Dust Deposition Along the Trans-Atlantic Transit Using the Decadelong Record of Aerosol Measurements from CALIOP, MODIS, MISR, and IASI. *J. Geophys. Res. Atmos.* **2019**, *124*, 7975–7996. [[CrossRef](#)]
5. Knippertz, P.; Todd, M.C. Mineral dust aerosols over the Sahara: Meteorological controls on emission and transport and implications for modeling. *Rev. Geophys.* **2012**, *50*, 2011RG000362. [[CrossRef](#)]
6. Washington, R.; Todd, M.C.; Engelstaedter, S.; Mbainayel, S.; Mitchell, F. Dust and the low-level circulation over the Bodélé Depression, Chad: Observations from BoDEx 2005. *J. Geophys. Res. Atmos.* **2006**, *111*, D03201. [[CrossRef](#)]
7. Lavaysse, C.; Flamant, C.; Evan, A.; Janicot, S.; Gaetani, M. Recent climatological trend of the Saharan heat low and its impact on the West African climate. *Clim. Dyn.* **2016**, *47*, 3479–3498. [[CrossRef](#)]
8. Marsham, J.H.; Hobby, M.; Allen, C.J.T.; Banks, J.R.; Bart, M.; Brooks, B.J.; Cavazos-Guerra, C.; Engelstaedter, S.; Gascoyne, M.; Lima, A.R.; et al. Meteorology and dust in the central Sahara: Observations from Fennec supersite-1 during the June 2011 Intensive Observation Period. *J. Geophys. Res. Atmos.* **2013**, *118*, 4069–4089. [[CrossRef](#)]
9. Schepanski, K.; Heinold, B.; Tegen, I. Harmattan, Saharan heat low, and West African monsoon circulation: Modulations on the Saharan dust outflow towards the North Atlantic. *Atmos. Chem. Phys.* **2017**, *17*, 10223–10243. [[CrossRef](#)]
10. Ali, E.; Xu, W.; Xie, L.; Ding, X. Assessment of Aeolian Activity in the Bodélé Depression, Chad: A Dense Spatiotemporal Time Series From Landsat-8 and Sentinel-2 Data. *Front. Environ. Sci.* **2022**, *9*, 808802. [[CrossRef](#)]
11. Fiedler, S.; Schepanski, K.; Heinold, B.; Knippertz, P.; Tegen, I. Climatology of nocturnal low-level jets over North Africa and implications for modeling mineral dust emission. *J. Geophys. Res. Atmos.* **2013**, *118*, 6100–6121. [[CrossRef](#)]
12. Chaboureaud, J.P.; Flamant, C.; Dauhut, T.; Kocha, C.; Lafore, J.P.; Lavaysse, C.; Marnas, F.; Mokhtari, M.; Pelon, J.; Reinares Martínez, I.; et al. Fennec dust forecast intercomparison over the Sahara in June 2011. *Atmos. Chem. Phys.* **2016**, *16*, 6977–6995. [[CrossRef](#)]

13. Redelsperger, J.-L.; Thorncroft, C.D.; Diedhiou, A.; Lebel, T.; Parker, D.J.; Polcher, J. African Monsoon Multidisciplinary Analysis: An International Research Project and Field Campaign. *Bull. Am. Meteorol. Soc.* **2006**, *87*, 1739–1746. [\[CrossRef\]](#)
14. Kalu, A.E. The African dust plume: Its characteristics and propagation across West Africa in winter. *SCOPE* **1979**, *14*, 95–118.
15. Herman, J.; Bhartia, P.; Torres, O.; Hsu, C.; Seftor, C.; Celarier, E. Global distribution of UV-absorbing aerosols from Nimbus 7/TOMS data. *J. Geophys. Res. Atmos.* **1997**, *102*, 16911–16922. [\[CrossRef\]](#)
16. Goudie, A.S.; Middleton, N.J. *Desert Dust in the Global System*; Springer Science & Business Media: Berlin/Heidelberg, Germany, 2006.
17. Brooks, N.; Legrand, M. Dust variability over northern Africa and rainfall in the Sahel. In *Linking Climate Change to Land Surface Change*; Springer: Berlin/Heidelberg, Germany, 2000; Volume 6, pp. 1–25.
18. Washington, R.; Todd, M.C. Atmospheric controls on mineral dust emission from the Bodélé Depression, Chad: The role of the low level jet. *Geophys. Res. Lett.* **2000**, *27*, L17701. [\[CrossRef\]](#)
19. Ben-Ami, Y.; Koren, I.; Rudich, Y.; Artaxo, P.; Martin, S.T.; Andreae, M.O. Transport of North African dust from the Bodélé depression to the Amazon Basin: A case study. *Atmos. Chem. Phys.* **2010**, *10*, 7533–7544. [\[CrossRef\]](#)
20. Lebel, T.; Parker, D.J.; Flamant, C.; Bourlès, B.; Marticorena, B.; Mougou, E.; Peugeot, C.; Diedhiou, A.; Haywood, J.M.; Ngamini, J.B.; et al. The AMMA field campaigns: Multiscale and multidisciplinary observations in the West African region. *Q. J. R. Meteorol. Soc.* **2010**, *136*, 8–33. [\[CrossRef\]](#)
21. Seity, Y.; Brousseau, P.; Malardel, S.; Hello, G.; Bénard, P.; Bouttier, F.; Lac, C.; Masson, V. The AROME-France Convective-Scale Operational Model. *Mon. Weather Rev.* **2011**, *139*, 976–991. [\[CrossRef\]](#)
22. Fourrié, N.; Nuret, M.; Brousseau, P.; Caumont, O.; Doerenbecher, A.; Wattrelot, E.; Moll, P.; Bénichou, H.; Puech, D.; Bock, O.; et al. The AROME-WMED reanalyses of the first special observation period of the Hydrological cycle in the Mediterranean experiment (HyMeX). *Geosci. Model Dev.* **2019**, *12*, 2657–2678. [\[CrossRef\]](#)
23. Kocha, C.; Tulet, P.; Lafore, J.P.; Flamant, C. The importance of the diurnal cycle of Aerosol Optical Depth in West Africa. *Geophys. Res. Lett.* **2013**, *40*, 785–790. [\[CrossRef\]](#)
24. Parajuli, S.P.; Stenchikov, G.L.; Ukhov, A.; Shevchenko, I.; Dubovik, O.; Lopatin, A. Aerosol vertical distribution and interactions with land/sea breezes over the eastern coast of the Red Sea from lidar data and high-resolution WRF-Chem simulations. *Atmos. Chem. Phys.* **2020**, *20*, 16089–16116. [\[CrossRef\]](#)
25. Hersbach, H.; Bell, B.; Berrisford, P.; Hirahara, S.; Horányi, A.; Muñoz-Sabater, J.; Nicolas, J.; Peubey, C.; Radu, R.; Schepers, D.; et al. The ERA5 global reanalysis. *Q. J. R. Meteorol. Soc.* **2020**, *146*, 1999–2049. [\[CrossRef\]](#)
26. Gelaro, R.; McCarty, W.; Suárez, M.J.; Todling, R.; Molod, A.; Takacs, L.; Randles, C.A.; Darmenov, A.; Bosilovich, M.G.; Reichle, R.; et al. The Modern-Era Retrospective Analysis for Research and Applications, Version 2 (MERRA-2). *J. Clim.* **2017**, *30*, 5419–5454. [\[CrossRef\]](#) [\[PubMed\]](#)
27. Buchard, V.; Randles, C.A.; da Silva, A.M.; Darmenov, A.; Colarco, P.R.; Govindaraju, R.; Ferrare, R.; Hair, J.; Beyersdorf, A.J.; Ziemba, L.D.; et al. The MERRA-2 Aerosol Reanalysis, 1980 Onward. Part II: Evaluation and Case Studies. *J. Clim.* **2017**, *30*, 6851–6872. [\[CrossRef\]](#)
28. Giles, D.M.; Sinyuk, A.; Sorokin, M.G.; Schafer, J.S.; Smirnov, A.; Slutsker, I.; Eck, T.F.; Holben, B.N.; Lewis, J.R.; Campbell, J.R.; et al. Advancements in the Aerosol Robotic Network (AERONET) Version 3 database—Automated near-real-time quality control algorithm with improved cloud screening for Sun photometer aerosol optical depth (AOD) measurements. *Atmos. Meas. Tech.* **2019**, *12*, 169–209. [\[CrossRef\]](#)
29. Evan, A.T.; Flamant, C.; Gaetani, M.; Guichard, F. The past, present and future of African dust. *Nature* **2016**, *531*, 493–495. [\[CrossRef\]](#)
30. Roberts, A.J.; Woodage, M.J.; Marsham, J.H.; Highwood, E.J.; Ryder, C.L.; McGinty, W.; Wilson, S.; Crook, J. Can explicit convection improve modelled dust in summertime West Africa? *Atmos. Chem. Phys.* **2018**, *18*, 9025–9048. [\[CrossRef\]](#)
31. Heinold, B.; Knippertz, P.; Marsham, J.H.; Fiedler, S.; Dixon, N.S.; Schepanski, K.; Laurent, B.; Tegen, I. The role of deep convection and nocturnal low-level jets for dust emission in summertime West Africa: Estimates from convection-permitting simulations. *J. Geophys. Res. Atmos.* **2013**, *118*, 4385–4400. [\[CrossRef\]](#)
32. Jury, M.R. Climatic modulation of early summer dust emissions over West Africa. *J. Arid Environ.* **2018**, *152*, 55–68. [\[CrossRef\]](#)
33. Cowie, S.M.; Knippertz, P.; Marsham, J.H. A climatology of dust emission events from northern Africa using long-term surface observations. *Atmos. Chem. Phys.* **2014**, *14*, 8579–8597. [\[CrossRef\]](#)
34. Wang, W.; Evan, A.T.; Lavaysse, C.; Flamant, C. The role the Saharan Heat Low plays in dust emission and transport during summertime in North Africa. *Aeolian Res.* **2017**, *28*, 1–12. [\[CrossRef\]](#)
35. Cook, K.H.; Vizy, E.K. Contemporary Climate Change of the African Monsoon Systems. *Curr. Clim. Change Rep.* **2019**, *5*, 145–159. [\[CrossRef\]](#)
36. Engelstaedter, S.; Washington, R.; Flamant, C.; Parker, D.J.; Allen, C.J.T.; Todd, M.C. The Saharan heat low and moisture transport pathways in the central Sahara—Multi-aircraft observations and Africa-LAM evaluation. *J. Geophys. Res. Atmos.* **2015**, *120*, 4417–4442. [\[CrossRef\]](#)

37. Francis, D.; Fonseca, R.; Nelli, N.; Cuesta, J.; Weston, M.; Evan, A.; Temimi, M. The Atmospheric Drivers of the Major Saharan Dust Storm in June 2020. *Geophys. Res. Lett.* **2020**, *47*, e2020GL090102. [[CrossRef](#)]
38. Bercos-Hickey, E.; Nathan, T.R.; Chen, S.-H. On the Relationship between the African Easterly Jet, Saharan Mineral Dust Aerosols, and West African Precipitation. *J. Clim.* **2020**, *33*, 3533–3546. [[CrossRef](#)]
39. Issa Lélé, M.; Lamb, P.J. Variability of the Intertropical Front (ITF) and Rainfall over the West African Sudan–Sahel Zone. *J. Clim.* **2010**, *23*, 3984–4004. [[CrossRef](#)]
40. Berry, G.; Reeder, M.J. Objective Identification of the Intertropical Convergence Zone: Climatology and Trends from the ERA-Interim. *J. Clim.* **2014**, *27*, 1894–1909. [[CrossRef](#)]
41. Dione, C.; Lohou, F.; Lothon, M.; Adler, B.; Babić, K.; Kalthoff, N.; Pedruzo-Bagazgoitia, X.; Bezombes, Y.; Gabella, O. Low-level stratiform clouds and dynamical features observed within the southern West African monsoon. *Atmos. Chem. Phys.* **2019**, *19*, 8979–8997. [[CrossRef](#)]
42. Strong, J.D.; Vecchi, G.A.; Ginoux, P. The climatological effect of Saharan dust on global tropical cyclones in a fully coupled GCM. *J. Geophys. Res. Atmos.* **2018**, *123*, 5538–5559. [[CrossRef](#)]

Disclaimer/Publisher’s Note: The statements, opinions and data contained in all publications are solely those of the individual author(s) and contributor(s) and not of MDPI and/or the editor(s). MDPI and/or the editor(s) disclaim responsibility for any injury to people or property resulting from any ideas, methods, instructions or products referred to in the content.